

Regular Article

# External Radiation Exposure to the Public Using Car-borne Survey Method in the Uranium and Thorium Bearing Region of Lolodorf, Cameroon

Guillaume Samuel Bineng<sup>1,2</sup>, Saïdou<sup>1,2\*</sup>, Masahiro Hosoda<sup>3</sup>, Yvette Flore Tchuenta Siaka<sup>2</sup>, Naofumi Akata<sup>4</sup>, Simplicie Feutseu Talla<sup>1</sup>, Patrice Ele Abiama<sup>2</sup> and Shinji Tokonami<sup>5</sup>

<sup>1</sup>Nuclear Physics Laboratory, Faculty of Science, University of Yaoundé I, P.O. Box 812 Yaoundé, Cameroon

<sup>2</sup>Nuclear Technology Section, Institute of Geological and Mining Research, P.O. Box 4110 Yaoundé, Cameroon

<sup>3</sup>Hirosaki University Graduate School of Health Sciences, Hirosaki City, Aomori, Japan

<sup>4</sup>National Institute for Fusion Sciences, 322-6 Oroshi, Toki, Gifu 509-5292, Japan

<sup>5</sup>Department of Radiation Physics, Institute of Radiation Emergency Medicine, Hirosaki University, Hirosaki City, Aomori 036-8564, Japan

Received 6 August 2019; revised 15 October 2019; accepted 8 November 2019

This study deals with natural radiation exposure to the public caused by external sources in seven inhabited areas located in the uranium and thorium bearing region of Lolodorf, Cameroon. The activity concentrations of <sup>238</sup>U, <sup>232</sup>Th, and <sup>40</sup>K were measured, the annual effective dose to the public assessed, and the distribution map of absorbed dose rate in air was performed. In-situ gamma spectrometry and car-borne survey method using the 3-in × 3-in NaI (TI) scintillation spectrometer were used. The average absorbed dose rates in air, the external effective dose and the activity concentrations in soil of <sup>238</sup>U, <sup>232</sup>Th and <sup>40</sup>K were  $50.4 \pm 7.2$  nGy h<sup>-1</sup>,  $0.33 \pm 0.05$  mSv y<sup>-1</sup>, and  $33 \pm 3$  Bq kg<sup>-1</sup>,  $53 \pm 9$  Bq kg<sup>-1</sup>,  $182 \pm 22$  Bq kg<sup>-1</sup> respectively. The ratios of the indoor dose rate to outdoor dose rate varied from  $0.86 \pm 0.04$  to  $1.12 \pm 0.67$  with a mean value of  $1.02 \pm 0.02$ . Compared to UNSCEAR limits, these radiological risk indicators are relatively high at certain points in the study area. Except for these points and their nearest neighborhood, soils can be used as building materials. In addition, high natural radiation areas are known and well located.

**Key words:** uranium, thorium, car-borne survey, absorbed dose rates in air

## 1. Introduction

The main cause of human external exposure to natural radioactivity is the uranium and thorium series, as well as <sup>40</sup>K. Soils, rocks and building materials contain radioactivity at varying levels by their mineralogical composition<sup>1</sup>. Car-borne survey and in-situ gamma spectrometry are common methods that have proven

effective in directly assessing the dose in the field. In recent decades, many research teams around the world have used these methods to quickly know the levels of radioactivity in a vast environment. This is the case in Brunei<sup>2</sup>, Turkey<sup>3</sup> and Japan<sup>4,5</sup> where several series of measurements of natural and artificial radioactivity were carried out.

In Cameroon, public exposure to natural radiation has been extensively studied. The study conducted by Ngachin *et al.*<sup>6</sup>, has revealed the occurrence of natural radioactivity in building materials. But, the level of this radioactivity is not harmful to the public according to the standards defined by the Organization for Economic Co-

\*Saïdou : Nuclear Technology Section, Institute of Geological and Mining Research, P.O. Box 4110 Yaoundé, Cameroon, P.O. Box 4110 Yaoundé, Cameroon  
E-mail: saidous2002@yahoo.fr

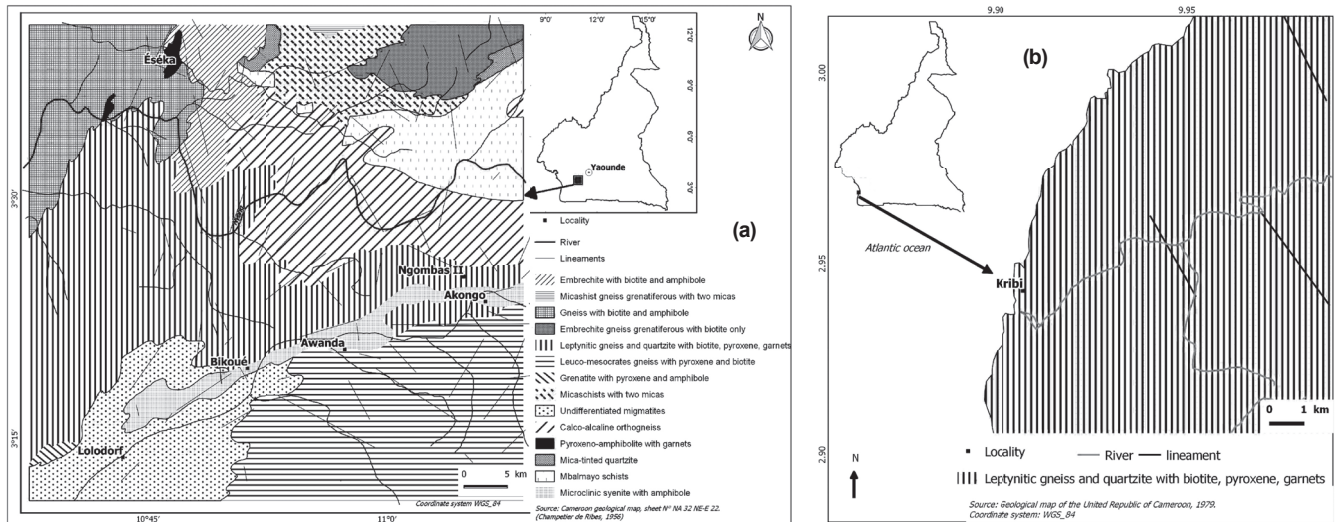


**Fig. 1.** Geological map of the seven study areas located in the uranium and thorium bearing region of Lolodorf in West-southern Cameroon: the localities of Akongo, Awanda, Bikoue, Eseka, Lolodorf and Ngombas in (a), and the locality of Kribi in (b).

operation and Development (OECD)<sup>7</sup>. In the uranium bearing region of Poli in northern Cameroon, most of the total dose evaluated is attributable to the inhalation of radon in homes and high levels of  $^{210}\text{Po}$  and  $^{210}\text{Pb}$  in vegetables and foodstuffs<sup>8</sup>. High radioactivity level was observed in soil samples due to the occurrence of uranium and thorium bearing radiogenic heavy minerals in the uranium and thorium bearing region of Lolodorf<sup>9</sup>. Radioactivity measurements in soil samples using gamma spectrometry in laboratory were performed by Ndjana Nkoulou II *et al.*<sup>10</sup> have shown that the concentrations of primordial radionuclides were high in some soil samples taken from five localities in the uranium and thorium bearing region of Lolodorf. Similar work has been done in Douala, the economic capital and one of the largest cities in Cameroon. The radioactivity found in the soil was high at certain points of the city<sup>11</sup>.

The current work is aimed at studying extensively natural radiation exposure to the public in the uranium and thorium bearing region of Lolodorf where are located high natural radiation areas. Activity concentrations of  $^{238}\text{U}$ ,  $^{232}\text{Th}$ ,  $^{40}\text{K}$ , and absorbed dose rates in air were carried out using *in-situ* gamma spectrometry and car-borne survey method. The database of the region was extended by studying the unexplored localities of Eseka, Akongo, Lolodorf and Kribi. These results were making possible the radiological mapping of the region.

## 2. Material and methods

### 2.1. Study areas

The uranium and thorium bearing region of Lolodorf as shown in Figure 1 (a and b) is located in the Western

Cameroon, respectively in the Ocean, the Nyong & So'o, and the Nyong & Kelle Divisions: Awanda (E10°59', N3°22'), Bikoue (E10°51', N3°21'), Kribi (E9°54', N2°57'), Lolodorf (E10°44'30", N3°14'), Akongo (E11°03', N3°14'), Eseka (E10°46'30", N3°39') and Ngombas (E11°06', N3°25') are all approximately located between 70 km to 340 km of Yaounde, Capital city of Cameroon. It belongs to the pan African chain of Central Africa, more exactly in the Yaounde-East and Yaounde-West groups<sup>12-14</sup>. Figure 1 (a and b) displays the presence of the syenite along the Akongo-Awanda-Bikoue corridor. In addition, there are the gneiss, the biotite and the quartzite in Ngombas, the south of Akongo and the north of Bikoue. The gneiss and biotite also cover the entire south of Awanda, a part of Eseka and much of its neighborhood. In Lolodorf, there is rather the undifferentiated migmatite. The limestone and various metamorphic rocks such as gneiss and Mbalmayo schists are also there. A detailed study of the elements in Figure 1 showed that essential minerals like potassic feldspars, micas, muscovite, microclines, migmatites are present in the Lolodorf region; as accessories, sphenes and monazites are also there, zircon, apatite and rutile are abundant<sup>13-15</sup>. The literature shows that some rocks such as syenite, granite, granulites, rhyolites, and plutonic can have the high U and Th content; radioactivity in diorites, basalts and gabbros is also significant. In sedimentary rocks, the black shale, gypsum and anhydrides contain U and Th; the U content is high into the limestone<sup>15-18</sup>. There is also radioactivity in sandstone, gravel, sand. Radioactivity may appear as an inclusion in the essential minerals, which are important constituents of rocks, or into accessory minerals. All the above-mentioned minerals are present in the soil and rock of the uranium

and thorium bearing region of Lolodorf<sup>13-15</sup>). The climate is equatorial; the West side is influenced by the proximity of the sea: that is to say, wetter than on the inner plateau at the same latitude. Temperatures range from 25 to 26°C with two dry seasons and two rainy seasons. The dry season is caused by a tropical continental air mass blowing from the Sahara Desert between December-February and July-August. The rainy season is brought by a tropical maritime air mass blowing from the Atlantic Ocean between September-November and March-June<sup>6, 13, 14</sup>. According to Central Bureau of the Census and Population Studies (CBCPS, 2004), population is about 164 829 inhabitants<sup>19</sup>.

## 2.2. Methodology

In the current work, the car-borne survey method and *in-situ* gamma spectrometry using the 3-in×3-in NaI (TI) scintillation spectrometer (EMF-211; EMF Japan Co. Japan) were used to estimate the radiation dose and the activity concentrations of <sup>238</sup>U, <sup>232</sup>Th and <sup>40</sup>K respectively. The field work was carried out in the studied areas from July 20<sup>th</sup> to 24<sup>th</sup> and August 1<sup>st</sup> to 2<sup>nd</sup> 2016. The methodology and the calibration of the equipment are well detailed by Minato<sup>20</sup> and Hosoda *et al.*<sup>21</sup> respectively. The detector, connected to a laptop for the controls, was placed inside the car (Land Cruiser TOYOTA) at about 1 m from the ground. The car was moving with an average speed of 40 km h<sup>-1</sup>. In order to determine the dose rate in the air outside the vehicle, the count rate measured inside has been corrected by multiplying it with a shielding factor. Due to the absorption of gamma rays by the car's body, a shielding factor was evaluated to convert the values measured inside the car into the ambient dose rate outside of the car at 10 points and correcting them with the inside counts rate. Count measurements were recorded over consecutive 30 s intervals during a total recording period of 2 min. Every 30 s the detection system, directly connected to a GPS, makes measurements, records the data along the road as well as the geographical coordinates of the different measuring points. When the absorbed dose rates in air is very high in an area, we get out of the car and at a specific point of the area, the 15min measurements is used just to determine the activity concentrations of the primordial radionuclides responsible for absorbed gamma dose rates. Measurements of gamma-ray pulse height distribution were carried outside the car 1 m above the ground surface for 15 min at 52 points. Activity concentrations of <sup>238</sup>U, <sup>232</sup>Th and <sup>40</sup>K in soil and their contribution to the absorbed dose rates in air were determined using the method developed by Minato *et al.*<sup>22</sup> and well detailed by Hosoda *et al.*<sup>21</sup> The statistical errors for absorbed dose rate in air and activity concentrations for <sup>40</sup>K, <sup>238</sup>U and <sup>232</sup>Th obtained using this method depend on the integral

air kerma at each measurement point<sup>23</sup>, and these were evaluated in this study as 2%, 2%, 6–8% and 4–5%, respectively.

The external effective dose can be obtained directly using the following equation:

$$E = D_{out} \times DCF \times T \times (Q_{in} \times R + Q_{out}) \times 10^6 \quad (1)$$

Where  $E$  is the external effective dose (mSv y<sup>-1</sup>),  $D_{out}$  is the average absorbed dose rates in air (nGy h<sup>-1</sup>),  $DCF$  is the dose conversion factor from the air kerma to the external effective dose to adults ( $0.748 \pm 0.007$  Sv Gy<sup>-1</sup>),  $T$  is 8,760 h (24 h×365 d),  $Q_{in}$  and  $Q_{out}$  are indoor and outdoor occupancy factors respectively, and  $R$  is the ratio of indoor dose rate to outdoor dose rate.

The  $DCF$  value used in this study was given by Moriuchi<sup>24</sup>, whereas  $R$  value has been obtained experimentally for natural gamma-ray in the studied areas in the current work. Outdoor and indoor ambient dose rate measurements were performed using *Graetz X5 DE* manufactured in Germany and operational in the ranges 48 keV - 1.3 MeV for energy and 1 μSv h<sup>-1</sup> - 20 mSv h<sup>-1</sup> for dose rate.

$DCF$ ,  $Q_{in}$  and  $Q_{out}$  are 0.7 Sv Gy<sup>-1</sup>, 0.6 and 0.4, respectively.

## 3. Results and Discussion

### 3.1. Shielding factor and dose rate conversion factor

Yield between the outside and inside count rates is the shielding factor. Its value was  $1.62 \pm 0.03$ . Dose conversion factor was evaluated as 0.002 (nGy h<sup>-1</sup>cpm<sup>-1</sup>); it is the relationship between absorbed dose rates in air (nGy h<sup>-1</sup>) evaluated using the 22×22 response matrix method and total count rate outside the car (cpm)<sup>22, 25</sup>. Its uncertainty was found to be 0.001; the decision coefficient  $R^2$  for dose conversion factors was 0.958.

Thus,  $D_{out}$  the absorbed dose rates 1 m above the ground surface at each measurement point can be estimated using the following equation:

$$D_{out} = 2N_{in} \times 1.62 \times 0.002 \quad (2)$$

In this study, the counts  $N_{in}$  inside the car were obtained by 30 s measurements using car-borne survey. Since the dose rate conversion factor was given as dose rate (nGy h<sup>-1</sup>) for counts per minute (cpm), it is necessary to double  $N_{in}$  in order to convert into the counts per minute.

### 3.2. Distribution of absorbed dose rates in air

The survey route and the variations of the outdoor gamma dose rates in air were mapped in (Fig. 2) using QGIS software. This map was drawn using 1402 data in the studied areas of the uranium and thorium bearing region of Lolodorf except Kribi. A heterogeneous

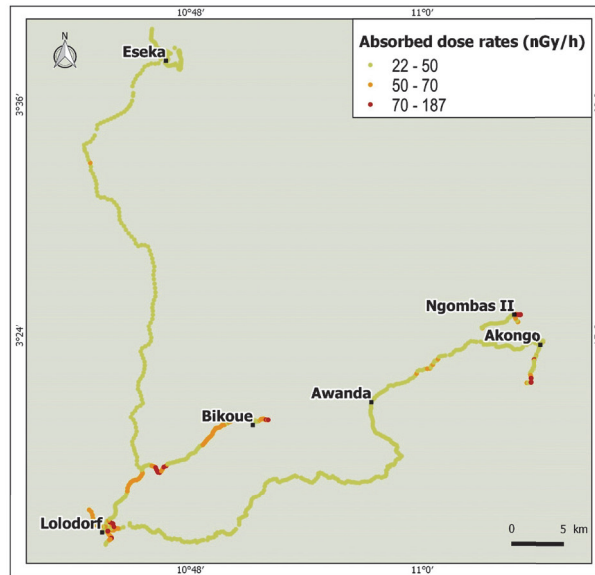


**Fig. 2.** Map showing the survey route and the variations of the outdoor gamma dose rates in the uranium and thorium bearing region of Lolodorf, except Kribi.

**Table 1.** Contributions of  $^{238}\text{U}$ ,  $^{232}\text{Th}$  and  $^{40}\text{K}$  to the absorbed dose rate in air in the studied areas of the uranium and thorium bearing region of Lolodorf

Area	N <sup>a</sup>	Absorbed dose rate (nGy h <sup>-1</sup> )			Total dose (nGy h <sup>-1</sup> )	Total dose range (nGy h <sup>-1</sup> )		Contribution to the absorbed dose rates (%)		
		$^{238}\text{U}$	$^{232}\text{Th}$	$^{40}\text{K}$		Min <sup>b</sup>	Max <sup>c</sup>	$^{238}\text{U}$	$^{232}\text{Th}$	$^{40}\text{K}$
Eseka	8	10.2 ± 0.7	14.8 ± 1.5	3.3 ± 0.2	28 ± 2	21 ± 2	35 ± 2	36.1	52.3	11.7
Ngombas	5	16.8 ± 4.6	37 ± 12	5.7 ± 0.7	60 ± 17	30 ± 1	105 ± 3	28.0	62.5	9.5
Awanda	6	8.3 ± 0.7	18.1 ± 1.4	4.6 ± 0.2	31 ± 2	25.3 ± 0.5	35.4 ± 0.7	26.6	58.4	15.0
Akongo	6	11.1 ± 1.1	29 ± 5	4.2 ± 0.1	44 ± 6	25.2 ± 0.5	69.6 ± 1.4	25.1	65.4	9.5
Lolodorf	3	14.8 ± 3.4	32.6 ± 7.3	7.3 ± 1.3	55 ± 2	32 ± 1	69.4 ± 1.4	26.8	59.2	14.0
Kribi	7	11.3 ± 3.8	22.5 ± 10.5	5 ± 1	39 ± 14	10.8 ± 0.2	114.6 ± 2.3	29.6	47.0	23.4
Bikoue	17	15.7 ± 3.3	43.8 ± 14.7	11.3 ± 2.2	71 ± 20	27.5 ± 0.6	357 ± 8	25.1	56.6	18.3
Average		13 ± 2	28 ± 6	6 ± 1	47 ± 8			28.2	57.3	14.5

<sup>a</sup>N is the number of data for each area; <sup>b</sup>Min: minimum value; <sup>c</sup>Max: maximum value

**Table 2.** Mean, median and range of  $^{238}\text{U}$ ,  $^{232}\text{Th}$  and  $^{40}\text{K}$  activity concentrations, absorbed dose rates in air and external effective doses in the studied areas of the uranium and thorium bearing region of Lolodorf

	Activity concentration (Bq kg <sup>-1</sup> )			Absorbed dose rate in air (nGy h <sup>-1</sup> )				EED <sup>f</sup> (mSv y <sup>-1</sup> )
	$^{238}\text{U}$	$^{232}\text{Th}$	$^{40}\text{K}$	$^{238}\text{U}$	$^{232}\text{Th}$	$^{40}\text{K}$	Total	
AM ± SD	33 ± 3	53 ± 9	182 ± 22	13 ± 2	28 ± 6	6 ± 1	47 ± 8	0.33 ± 0.05
GM (GSD)	28 ± 1	38 ± 1	150 ± 1	11 ± 2	22 ± 6	5.6 ± 0.8	40 ± 8	0.26 ± 0.69
Median	26	34	128	10	19.5	5.6	34.5	0.29
Minimum	6 ± 1	6 ± 1	79 ± 2	3 ± 1	4 ± 1	3 ± 1	11 ± 1	0.07 ± 0.01
Maximum	158 ± 11	450 ± 23	841 ± 17	62 ± 2	263 ± 6	31 ± 1	357 ± 8	2.37 ± 0.05

<sup>a</sup>AM : Arithmetic mean ; <sup>b</sup>GM : geometric mean ; <sup>c</sup>SD: standard deviation; <sup>d</sup>GSD: geometric standard deviation EED<sup>f</sup>: Annual effective dose

distribution of absorbed dose rates in air 1m above the ground was seen. The doses range from 70 to 185 nGy h<sup>-1</sup> in the north of Akongo, east of Ngombas and in some places along the Bikoue, Awanda, Lolodorf corridor. Elsewhere, the dose was relatively lower than the world average value of 59 nGy h<sup>-1</sup> (UNSCEAR)<sup>1</sup>. Those

variations could be explained by the fact that, ground, rock and bedrock were not homogeneous in the whole region. Moreover, the geological intrusions such as lineaments could also justify this behavior of the absorbed dose rate.

Table 1 displays the mean contributions of  $^{238}\text{U}$ ,  $^{232}\text{Th}$

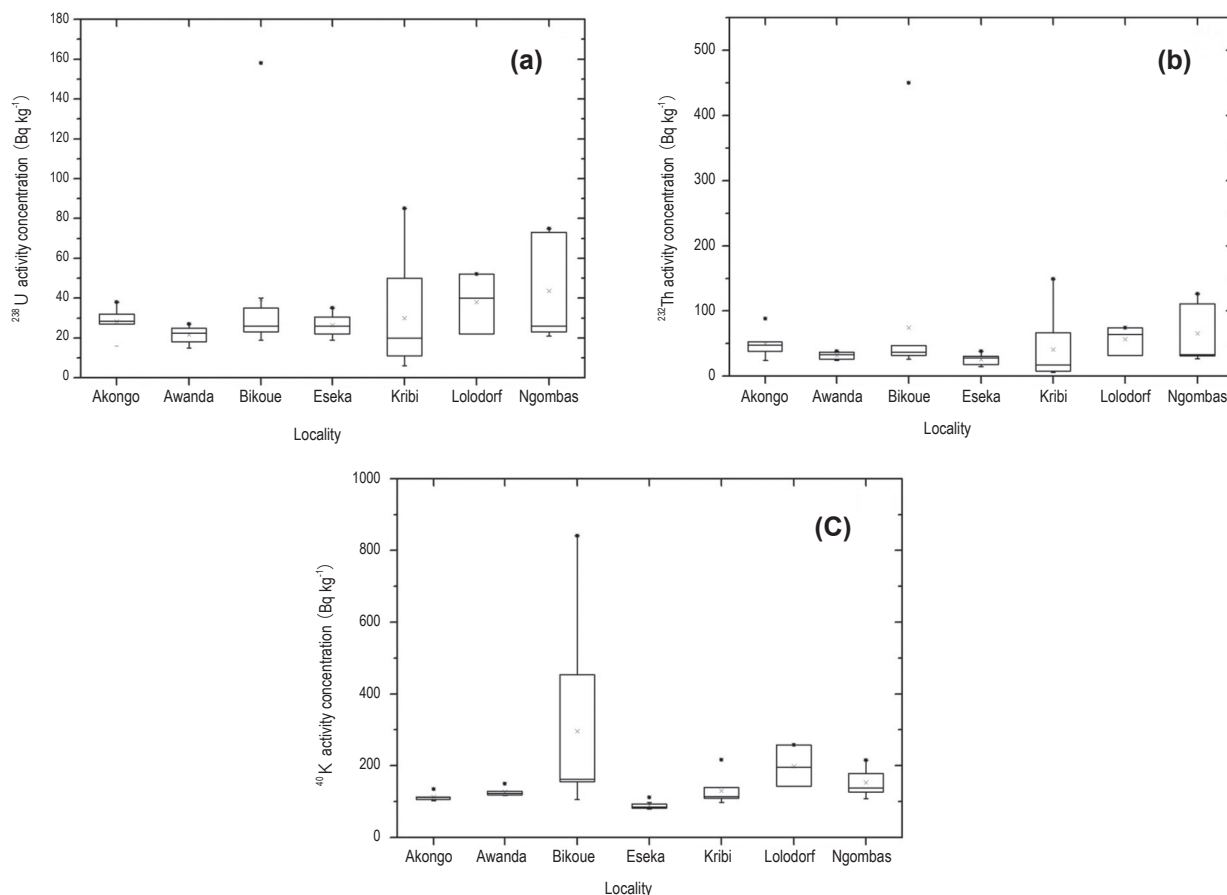


**Fig. 3.** Activity concentrations of  $^{238}\text{U}$ ,  $^{232}\text{Th}$  and  $^{40}\text{K}$  in the seven study areas of the uranium and thorium bearing region of Lolodorf.

and  $^{40}\text{K}$  to the absorbed dose rate in air for the seven inhabited areas.  $^{232}\text{Th}$  contribution to the absorbed dose rate was higher than those of  $^{238}\text{U}$  and  $^{40}\text{K}$ . The mean absorbed dose rates in air of each of the studied areas are also listed in Table 1. The average values of absorbed gamma dose rates in air varied from 11  $\text{nGy h}^{-1}$  (Kribi at the beach, N2.923175, E9.900265) to 357  $\text{nGy h}^{-1}$  (Bikoue, N3.327398, E10.867035), with a mean value of 47  $\text{nGy h}^{-1}$ . This mean value was lower than the world average value of 59  $\text{nGy h}^{-1}$  (UNSCEAR)<sup>1</sup>. It can be seen in Table 1 that, two of the studied areas had a mean value higher than the world average value of 59  $\text{nGy h}^{-1}$ .

Compared with other studies in the world, the average value of 47  $\text{nGy h}^{-1}$  obtained for the uranium and thorium region of Lolodorf was very lower than 227.8  $\text{nGy h}^{-1}$  and 153  $\text{nGy h}^{-1}$  measured from the soil samples collected respectively at three beaches in Safaga, Egypt<sup>26</sup>, and at the border of the “Baie des Français”, Antsiranana, Madagascar<sup>27</sup> in Africa. In Japan, Inoue *et al.*<sup>28</sup> detailed data of absorbed dose rates in air in metropolitan Tokyo before the accident of the Fukushima Daiichi Nuclear Power Plant using car-borne survey; the mean value 49  $\pm$

6  $\text{nGy h}^{-1}$  observed was higher than the value obtained in this work.

### 3.3. Activity concentrations of $^{238}\text{U}$ , $^{232}\text{Th}$ and $^{40}\text{K}$

Figure 3 displays the box plot graphs which show median, 25 percentile, 75 percentile, maximum, and minimum values of  $^{238}\text{U}$ ,  $^{232}\text{Th}$  and  $^{40}\text{K}$  activity concentrations in each study area. Arithmetic and geometric means, median, minimum and maximum activity concentrations of  $^{238}\text{U}$ ,  $^{232}\text{Th}$  and  $^{40}\text{K}$  in the soil for the whole study area are displayed in Tables 2. Activity concentrations of  $^{238}\text{U}$ ,  $^{232}\text{Th}$  and  $^{40}\text{K}$  varied from  $6 \pm 1$  to  $158 \pm 11$  with an average of  $33 \pm 3 \text{ Bq kg}^{-1}$ ,  $6 \pm 1$  to  $450 \pm 23$  with an average of  $53 \pm 9 \text{ Bq kg}^{-1}$  and  $79 \pm 2$  to  $841 \pm 17$  with an average of  $182 \pm 22 \text{ Bq kg}^{-1}$ , respectively. The mean values of  $^{238}\text{U}$ ,  $^{232}\text{Th}$  and  $^{40}\text{K}$  in the earth's crust were 35, 30 and 400  $\text{Bq kg}^{-1}$  (UNSCEAR)<sup>1</sup>. However, in Figure 3, it can be seen from Bikoue that, the value of  $^{40}\text{K}$  is higher than 400  $\text{Bq kg}^{-1}$  in five points:  $473 \pm 9 \text{ Bq kg}^{-1}$  at (N3.32246, E10.826437),  $454 \pm 9 \text{ Bq kg}^{-1}$  at (N3.326707, E10.855557),  $602 \pm 12 \text{ Bq kg}^{-1}$  at (N3.3272, E10.866825),  $701 \pm 14 \text{ Bq kg}^{-1}$  at (N3.32743, E10.866988) and  $841 \pm 17 \text{ Bq kg}^{-1}$  at (N3.327398,

E10.867035). This last value observed in Bikoue area was two times higher than the world average value.

Activity concentration of  $^{238}\text{U}$  found in Ngombas, Kribi and Bikoue are higher than the world average value of  $35 \text{ Bq kg}^{-1}$ . But, it can be seen from Figure 3 some points which have values 2-5 times higher than the world average one. High concentration of  $^{238}\text{U}$  observed in this study area can be explained by the occurrence uranium bearing radiogenic heavy minerals<sup>9)</sup>. Compared to the value of  $35 \text{ Bq kg}^{-1}$  above, it can be seen in Figure 3 that,  $^{238}\text{U}$  average activity concentrations in the ground were low in Akongo, Awanda and Eseka. This is consistent since the uranium and thorium mining activities have not yet started; Eseka is not identified as a potential uranium or thorium mining site. Therefore, radioactivity in these studied areas can be classified into high-level, mid-level and low-level background radiation.

In this study, 67.3% (35 over 52) of the measurement points have activity concentration of  $^{232}\text{Th}$  2-15 times higher than the world average value of  $30 \text{ Bq kg}^{-1}$  (UNSCEAR<sup>1)</sup>). In Eseka, this activity concentration is the lowest. Correlation between uranium and thorium in soil under investigation for the major studied areas is good (correlation coefficient is 0.83).

In the previous section titled “study areas”, it is shown that the bedrock of the uranium and thorium bearing region of Lolodorf consists of many rocks and minerals which have the high U, Th and K content. But under the excessive action of heat and pressure, the rocks of that bedrock eventually crack causing the circulation of hot water or vapors underground. The intensification of this phenomenon can lead to the dissolution of many elements and induce their migration to the empty zones formed by these cracks. The nature of the crystals thus formed depends on the composition of the initial rock. Under the action of erosion, precipitation, winds, soil structure and reservoir rock, this natural radioactivity will migrate to the soil surface. In situ gamma spectrometry of the soil at a similar location will obviously reveal high levels of natural radioactivity. In addition, some studies have shown that the area has a significant uranium and thorium potential<sup>9, 15)</sup>. It is this set of elements that can justify these low, medium and high values of the specific activities of U, Th and K at certain points of the current study areas.

Compared to the average values of  $24 \pm 1 \text{ Bq kg}^{-1}$  for  $^{238}\text{U}$ ,  $28 \pm 1 \text{ Bq kg}^{-1}$  for  $^{232}\text{Th}$  and  $506 \pm 3 \text{ Bq kg}^{-1}$  for  $^{40}\text{K}$  determined in the uranium bearing region of Poli, by Saïdou *et al.*<sup>8)</sup> using gamma spectrometry measurements of soil samples in laboratory, these different values are all lower than the one determined within the framework of the current study except  $^{40}\text{K}$  which is about three times higher. Activity concentrations of 160, 480 and 1050  $\text{Bq kg}^{-1}$  for  $^{238}\text{U}$ ,  $^{232}\text{Th}$  and  $^{40}\text{K}$  obtained by Ele Abiama

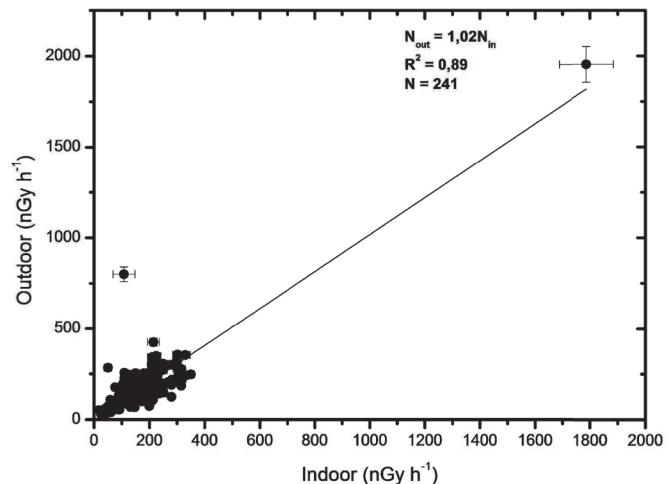


Fig. 4. Ratio of indoor to outdoor dose rates in the seven studied areas of the uranium and thorium bearing region of Lolodorf.

*et al.*<sup>9)</sup> using gamma spectrometry measurements of soil samples in laboratory, in the same region of Lolodorf (Awanda, Ngombas and Bikoue) are highest. Difference observed between in-situ and laboratory measurements could be explained by the fact that in-situ gamma spectrometry gives representative source concentration in the horizontal plane while gamma spectrometry measures radioactivity in soil sample collected from a  $1 \text{ m}^2$  area. According to Ele Abiama *et al.*<sup>9)</sup>, these highest activity concentrations of  $^{238}\text{U}$ ,  $^{232}\text{Th}$  and  $^{40}\text{K}$  in the above areas could be explained by the fact that most of the sampled points are located in the zones identified with uranium and thorium anomalies in the studied area. One should note that the world average values of the activity concentrations ( $^{238}\text{U}$ ,  $^{232}\text{Th}$  and  $^{40}\text{K}$ ) used for comparison in the present study were estimated by UNSCEAR<sup>1)</sup> using natural radiation survey data from countries including uranium and thorium mining regions, although they are not well represented.

### 3.4. External effective dose assessment

The average external effective doses of the entire study area are displayed in Table 2. The mean value in this study is lower than the world average value of  $0.5 \text{ mSv y}^{-1}$  (UNSCEAR<sup>1)</sup>).

Compared with other studies in Cameroon, external effective dose in this study is lower than  $0.6 \text{ mSv y}^{-1}$ ,  $0.41 \text{ mSv y}^{-1}$  and  $0.42 \text{ mSv y}^{-1}$  determined respectively in Poli by Saïdou *et al.*<sup>8)</sup>, in Awanda, Ngombas and Bikoue by Ele Abiama *et al.*<sup>9)</sup> using gamma spectrometry of soil samples in laboratory, in Douala by Takoukam Soh *et al.*<sup>11)</sup> using car-borne survey method.

In Japan, the average value of  $0.32 \text{ mSv y}^{-1}$  obtained by Inoue *et al.*<sup>27)</sup> in Metropolitan Tokyo before the accident of the Fukushima Daiichi Nuclear Power Plant, using car-

borne survey method is more equal to the value measured in the present work.

The materials used for most of building constructions also contain radionuclides. The average factor  $R$  of  $1.02 \pm 0.02$  experimentally obtained in the entire studied area was applied to take into account their contribution in the external dose estimation. Figure 4 showed the ratio of indoor dose rate to outdoor dose rate in 241 houses in the seven studied areas.

The slope of this regression line was used as the factor above. In Eseka, Ngombas, Awanda, Akongo, Lolodorf, Kribi and Bikoue inhabited areas, these ratios were  $0.89 \pm 0.04$ ,  $0.98 \pm 0.04$ ,  $0.95 \pm 0.05$ ,  $1.11 \pm 0.67$ ,  $0.93 \pm 0.05$ ,  $0.86 \pm 0.04$  and  $1.12 \pm 0.42$  respectively. These different values are all higher than 0.6 and lower than 2.0, which are the boundary world values<sup>1)</sup>.

#### 4. Conclusion

The car-borne survey was performed in the uranium and thorium bearing region of Lolodorf, located in West-southern Cameroon to study natural radiation exposure to the public caused by external sources. This work was achieved by measuring the activity concentrations of  $^{238}\text{U}$ ,  $^{232}\text{Th}$  and  $^{40}\text{K}$ , the air kerma rates followed by external effective dose to the public assessment in the studied areas. Absorbed dose rates in air higher than  $60 \text{ nGy h}^{-1}$  were observed in the high natural radiation areas of Ngombas and Bikoue. Average activity concentration of  $^{40}\text{K}$  was found to be lower than the world average value while  $^{238}\text{U}$  and  $^{232}\text{Th}$  were found to be higher than the corresponding world average values. External effective dose was  $0.33 \text{ mSv y}^{-1}$  less than the world average value of  $0.5 \text{ mSv y}^{-1}$ . This study made possible the production of a radiological map of the region. The high natural radiation areas are now well located. These data were used to select inhabited areas for radon, thoron and thoron progeny measurements indoors. Results will shortly be reported.

#### Acknowledgements

This work was supported by JSPS KAKENHI Grant Number 26305021 and by the Institute of Geological and Mining Research (BIP 2016).

#### Conflict of Interest

The authors declare that the research was conducted in the absence of any commercial or financial relationships that could be construed as a potential conflict of interest.

#### References

1. UNSCEAR. UNSCEAR 2000 REPORT Vol. II: Sources and effects of ionizing radiation. United Nations Scientific Committee on the Effects of Atomic Radiation. New York: United Nations; 2000.
2. Lai K, Hu S, Kodairi K and Minato S. A car-borne survey of terrestrial gamma-ray dose rates in Brunei Darussalam. *Radioisotopes*. 1996;45:696–9.
3. Turhan S, Arikan IH, Oğuz F, Özdemir T, Yüce B, Varinlioğlu A and Köse A. Car-borne survey of natural background gamma dose rate in Çanakkale Region, Turkey. *Radiat Prot Dosim*. 2012;148(1):45–50.
4. Hosoda M, Tokonami S, Sorimachi A, Monzen S, Osanai M, Yamada M, Kashiwakura I and Akiba S. The time variation of dose rate artificially increased by the Fukushima nuclear crisis. *Sci Reports*. 2011;1:87.
5. Inoue K, Arai M, Fujisawa M, Saito K and Fukushi M. Detailed Distribution Map of Absorbed Dose Rate in Air in Tokatsu Area of Chiba Prefecture, Japan, Constructed by Car-Borne Survey 4 Years after the Fukushima Daiichi Nuclear Power Plant Accident. *PLoS ONE*. 2017;12:1.
6. Ngachin M, Garavaglia M, Giovani C, Kwato Njock MG and Nourreddine A. Assessment of natural radioactivity and associated radiation hazards in some Cameroonian building materials. *Radiat Meas*. 2007;42:61–7.
7. Organization for Economic Cooperation and Development criterion1979.
8. Saïdou, Bochud FO, Baechler S, Kwato Njock MG, Ngachin M and Froidevaux P. Natural radioactivity measurements and dose calculations to the public: case of the uranium-bearing region of Poli in Cameroon. *Radiat Meas*. 2011;46:254–60.
9. Ele Abiama P, Owono Ateba P, Ben-Bolie GH, Ekobena Fouda HP and El Khoukhi T. High background radiation investigated by gamma spectrometry of the soil in the southwestern region of Cameroon. *J Environ Radioact*. 2010;101:739–43.
10. Ndjana Nkoulou II JE, Feutseu Talla S, Bineng GS, Manga A, Tchuente Siaka YF and Saïdou. Natural radioactivity measurements in soil, external dose and radiological hazard assessment in the uranium and thorium bearing region of Lolodorf, Cameroon. *RADIOISOTOPES* 2018;67:435–46.
11. Takoukam Soh SD, Saïdou, Hosoda M, Ndjana Nkoulou II JE, Akata N, Bouba O and Tokonami S. Natural radioactivity measurements and external dose estimation by car-borne survey in Douala city, Cameroon. *Radioprotection*. 2018;53:255–63.
12. MINTP, MINTP 2016 Rapport final : Actualisation du tableau des distances interurbaines du Cameroun. Rapport Final, avril 2016. (Accessed 2019 Oct 6).
13. Champetier De Ribes G and Aubague M. Carte géologique de reconnaissance à l'échelle 1/500000 : Notice explicative sur la feuille de Yaoundé-Est. Paris: BRGM; 1956.
14. Champetier De Ribes G and Reyre D. Carte géologique de reconnaissance à l'échelle 1/500000 : Notice explicative sur la feuille Yaoundé-Ouest. Paris: BRGM; 1959.
15. Braun JJ. Comportement géochimique et minéralogique des terres rares, du thorium et de l'uranium dans le profilé latéritique d'Akongo (sud-ouest Cameroun). Thèse, Université de Nancy I: 1991.
16. Andráš P, Dirner V, Harnakova A. Determination of  $^{238}\text{U}$ ,  $^{232}\text{Th}$  and  $^{40}\text{K}$  activity in the rocks used in civil engineering from the Male Karpaty MTS. *Carpat J of Earth Environ Sci*. 2011;6 (1):5–14.
17. Mekongtso Nguelem EJ, Moyo Ndontchueng M, Motapon O. Determination of  $^{226}\text{Ra}$ ,  $^{232}\text{Th}$ ,  $^{40}\text{K}$ ,  $^{235}\text{U}$  and  $^{238}\text{U}$  activity concentration and public dose assessment in soil samples from bauxite ore deposits in western Cameroon. *Springer plus*. 2016;5(1):1253.
18. Beyala Ateba JF, Owono Ateba P, Ben-Bolie GH, Ekobena Fouda H, Ele Abiama P, Abega CR, Mvondo S. Determination of uranium

- in rocks and soil of south Cameroon by gamma spectrometry. *Radioisotopes*. 2011;60:10.
19. CBCPS. 2004 Census of Population of Cameroon. 3<sup>rd</sup> General Census of Population and Housing. Central Bureau of the Census and Population Studies; 2005. (Accessed 2016 May 25).
  20. Minato S. Vehicle-borne survey techniques for background radiations. Rep Governmental Industrial Research Institute, Nagoya, 1995;44:609–628.
  21. Hosoda M, Tokonami S, Omori Y, Sahoo SK, Akiba S, Sorimachi A, *et al.* Estimation of external dose by car-borne survey in Kerala, India. *PLoS ONE*. 2015;10(4).
  22. Minato S. A response matrix of a 3"  $\phi$   $\times$  3" NaI(Tl) scintillator for environmental gamma radiation analysis. Rep Governmental Industrial Research Institute, Nagoya 1978;27:384–397.
  23. Matsuda H, Minato S and Pasquale V. Evaluation of accuracy of response matrix method for environmental gamma ray analysis. *Radioisotopes*. 2002;51:42–50.
  24. Moriuchi S, Tsutsumi M, Saito K. Examination on conversion factors to estimate effective dose equivalent from absorbed dose in air for natural gamma radiations. *Jpn J Health Phys*. 1990; 25:121–128. (Japanese with English abstract)
  25. Minato S. Diagonal elements fitting technique to improve response matrixes for environmental gamma ray spectrum unfolding. *Radioisotopes*. 2001;50:463–71.
  26. Uosif MA, El-Taher A, Abbady GA. Radiological significance of beach sand used for climatotherapy from Safaga, Egypt, *Radiat Prot Dosim*. 2008;131:331–9.
  27. Kall B, Tombo T, Rasolonirina M, Rabesiranana N and Ambolamanana G. Contribution à l'étude de dose due à la radioactivité gamma du sol sur la rive de la baie des français, Antsiranana, Madagascar. *Afr Sci*. 2015;11:122–35.
  28. Inoue K, Hosoda M, Fukushi M, Furukawa M and Tokonami S. Absorbed dose rate in air in metropolitan Tokyo before the Fukushima Daiichi Nuclear Power Plant Accident. *Radiat Prot Dosim*. 2015; 167(1-3):231–4.